Pediatric Health, Medicine and Therapeutics

Dovepress
Taylor & Francis Group

Open Access Full Text Article

ORIGINAL RESEARCH

Pyroptosis-Related Molecular Clusters and Immune Infiltration in Pediatric Sepsis

Mingxin Lin[1,*], Chenxi Li[1,*], Ye Wang[1], Jingping Liu[2], Huiming Ye[1]

[1]Department of Laboratory Medicine, Fujian Key Clinical Specialty of Laboratory Medicine, Women and Children's Hospital, School of Medicine, Xiamen University, Xiamen, Fujian, People's Republic of China; [2]Department of Laboratory Medicine, The First Affiliated Hospital of Nanjing Medical University, Nanjing, People's Republic of China

*These authors contributed equally to this work

Correspondence: Jingping Liu, Department of Laboratory Medicine, The First Affiliated Hospital of Nanjing Medical University, No. 300 Guangzhou Road, Nanjing City, Jiangsu Province, People's Republic of China, Tel +86-15950530983, Email 15950530983@163.com; Huiming Ye, Department of Laboratory Medicine, Fujian Key Clinical Specialty of Laboratory Medicine, Women and Children's Hospital, School of Medicine, Xiamen University and Associate Professor of Laboratory Medicine, School of Public Health, Xiamen University, No. 10 Zhenhai Road, Xiamen City, Fujian Province, People's Republic of China, Tel +86-592-2662071, Email yehuiming@xmu.edu.cn

Background: Pediatric sepsis is a complex and heterogeneous condition resulting from a dysregulated immune response to infection. Pyroptosis, a newly recognized form of programmed cell death, has been implicated in the progression of various inflammatory diseases. However, the role of pyroptosis-related genes in pediatric sepsis remains unclear.

Methods: Based on the GSE13904 dataset, we explored the pyroptosis-related differentially expressed genes (DEGs) in pediatric sepsis. We analyzed the molecular clusters based on pyroptosis-related DEGs. The WGCNA algorithm was performed to identify cluster-specific DEGs. The optimal machine model was identified by multiple machine learning methods (RF, SVM, GLM, XGB). The diagnostic value of hub genes in pediatric sepsis was verified in the training (GSE13904) and validation set (GSE26440) through ROC. qRT-PCR was used to verify the expression levels of 5 hub genes in whole blood between the pediatric sepsis and the control.

Results: The dysregulated pyroptosis-related DEGs were identified in pediatric sepsis. Three pyroptosis-related molecular clusters were determined in pediatric sepsis. SVM presented the best discriminative performance with relatively lower residual and root mean square error. The nomogram, calibration curve, and decision curve analysis indicated the accuracy of SVM model to predict pediatric sepsis. 5 hub genes based on SVM presented satisfactory performance in the training and validation sets. These hub genes expression levels in pediatric sepsis were significantly higher than those in healthy controls in clinical samples.

Conclusion: Our study systematically analyzed the relationship between pyroptosis and pediatric sepsis, and constructed a promising predictive model to evaluate the risk of pediatric sepsis.

Keywords: pediatric sepsis, pyroptosis, molecular clusters, immune infiltration, machine learning, prediction model

Introduction

Sepsis is a life-threatening condition defined as organ dysfunction resulting from a dysregulated host response to pathogenic infection, and it remains a significant cause of high morbidity, mortality, and disease burden in pediatric population.[1–3] There were an estimated 48.9 million cases of sepsis and 11 million sepsis-related deaths worldwide. More than half of all sepsis cases occurred among pediatric population, resulting in 2.9 million sepsis-related deaths among children younger than 5 years, and 454,000 among children and adolescents aged 5–19 years.[4] In the pediatric population, sepsis is a complicated and dangerous condition that can progress rapidly to septic shock and death without timely and effective intervention. Thus, early diagnosis of sepsis and timely administration of antibiotics can significantly improve outcomes.[5–7] Unfortunately, given the clinical heterogeneity and complexity of sepsis,[8] there are no effective biomarkers for early diagnosis of sepsis. Therefore, more reliable novel biomarkers are urgently required for early sepsis recognition.

Received: 25 February 2025
Accepted: 20 August 2025
Published: 10 September 2025

Pyroptosis is a novel type of programmed cell death, also known as inflammatory programmed cell death.[9] There are four different signaling pathways have been identified to induce pyroptosis, including canonical inflammasome pathways, non-canonical inflammasome pathways, apoptotic caspases-mediated pathway, and granzymes-based pathway.[10] When pyroptosis occurs, cytoplasmic membrane pores formation, cells swell and lysis, and release pro-inflammatory cytokines, such as interleukin-1β (IL-1β) and interleukin-18 (IL-18).[3,11] Pyroptosis plays an essential role in host defense against pathogenic infection through the release of pro-inflammatory cytokines and cell lysis. However, excessive pyroptosis leads to dysregulated inflammatory response and cell or tissue damage, and may be involved in the pathological progression of many inflammatory diseases, including sepsis.[10,12,13] Recent studies have confirmed that pyroptosis plays an important role in the occurrence and development of sepsis. Caspase-11-dependent macrophage pyroptosis is critical for induction of septic shock in mice.[14,15] In the early hyper-inflammatory state of sepsis, excessive neutrophil pyroptosis is harmful because neutrophils are the main source of IL-1β during the infection. And caspase-1/11 knockout and IL-1β/IL-18 knockout can improve the survival rate in septic shock mice model.[16] Some evidence shows that NLRP3 inflammasome-induced pyroptosis contributes to age-related diseases and aging processes, indicating that pyroptotic activity is modulated by developmental stage. Furthermore, a single-cell RNA sequencing (scRNA-seq) study of human ovaries at different reproductive ages demonstrated that pyroptosis pathway activation increases with age, primarily in macrophages. These findings suggest that pyroptosis signaling is dynamically regulated during immune system maturation.[17,18] Although many studies have shown that inhibiting pyroptosis is helpful in the treatment of sepsis, there are also some studies have shown that activation of pyroptosis plays a protective role in sepsis. Therefore, pyroptosis functions as a "double-edged sword" in sepsis.[19] Although the role of pyroptosis in infectious diseases has garnered increasing attention in recent years, its molecular mechanisms and immunological regulatory pathways in pediatric populations remain insufficiently explored.

To address this gap, our study adopts a novel approach by focusing on pyroptosis-related genes as the analytical starting point. We employed unsupervised clustering to perform molecular subtyping of pediatric sepsis patients, aiming to uncover potential immune heterogeneity. Based on this, we further applied multiple machine learning algorithms to identify key feature genes and to construct clinically relevant biomarker panels. Unlike previous studies that largely focused on single indicators or adult samples, our integrative strategy provides a comprehensive framework—from molecular classification to the identification of diagnostic markers. This work offers new insights into the role of pyroptosis in pediatric sepsis and may contribute to early diagnosis and the development of personalized therapeutic strategies.

Materials and Methods

Microarray Dataset Collection and Data Process

Two microarray datasets (GSE13904 and GSE26440) related to pediatric sepsis were downloaded from GEO (www.ncbi.nlm.nih.gov/geo). The search keywords were "sepsis" and "children" with the following searching strategies: ((("sepsis"[All Fields]) AND "children"[All Fields]) AND "Homo sapiens"[organism]) AND "Expression profiling by array"[Filter]. Finally, GSE13904 (as training set) and GSE26440 (as validation set) were obtained. After being standardized, annotated, and cleared, the date from GSE13904 and GSE26440 dataset were used for bioinformatic analysis.

Identification of Pyroptosis-Related Differentially Expressed Genes (DEGs)

Pyroptosis-related expressed genes were screened from relevant literatures.[20–23] Subsequently, pyroptosis-related DEGs between pediatric sepsis and healthy controls were analyzed using the "limma" package in R software (version 4.2.1, the same below) based on p value < 0.05 and FC (fold changes) > 1.5. The boxplot and heat map were drawn to visualize the pyroptosis-related DEGs using "ggboxplot" and "pheatmap" packages, respectively.

Evaluation of the Immune Cell Infiltration

The CIBERSORT algorithm (https:/cibersort.stanford.edu/) was used for calculating the relative abundances of 22 types of immune cells in GSE13904 dataset. Only samples with p-values < 0.05 were considered accurate immune cell fractions, which were used for further analysis.

Unsupervised Clustering of Pediatric Sepsis

In order to further construct pyroptosis-related sepsis subtypes, we first utilized the Consensus Cluster Plus R package to identify the optimal cluster number based on pyroptosis-related DRGs expression profiles, then pediatric sepsis samples were classified into different clusters by using the k-means algorithm with 1,000 iterations. Finally, we chose the optimal cluster subtype number k = 3 based on the cumulative distribution function (CDF) curve, consistent cluster score (> 0.9), and consensus matrix.

Gene Set Variation Analysis (GSVA)

GSVA was performed to explain the differences in enriched gene sets among different clusters using the R package of "GSVA". The "limma" R package was used to analyze the differentially expressed pathways and biological functions in different clusters by GSVA scores. The t value>2 was considered as statistically significant.

Weighted Gene Co-Expression Network Analysis (WGCNA)

We calculated the variance of each gene based on gene expression profile, and selected the top 25% genes with the highest variance to further analysis. The goodSamplesGenes method of R Package was utilized to removed outlier samples. Furthermore, we also built a scale-free co-expression network by WGCNA and then determined soft threshold through using scale-free co-expression network. We selected an optimal soft threshold to construct the adjacency matrix and further converted it into a topological overlap matrix (TOM) for average link hierarchical clustering. Besides, we also used TOM to classify related modules to ensure that the number of genes in each module was not less than 50, and Similar modules were merged based on shear height 0.25 of gene module. The relevance between merge modules and subtypes was explored by Pearson. Similar methods constructed co-expression networks of disease and their subtypes, then we extracted the common genes of the two modules and took their intersection.

Gene Functional Enrichment Analysis

Gene ontology (GO) enrichment and Kyoto Encyclopedia of Genes and Genomes (KEGG) were conducted to analyze the possible biological functions of cluster-specific DEGs through ClusterProfiler software package and ggplot2 software package.

Construction of Predictive Model Based on Multiple Machine Learning Methods

Based on cluster-specific DRGs, we used the "caret" R packages for establishing machine learning models, including random forest model (RF), support vector machine model (SVM), generalized linear model (GLM), and eXtreme Gradient Boosting (XGB). RF is a kind of ensemble machine learning approach, which predicts classification or regression via a variety of independent decision trees. SVM generates a hyperplane in the feature space with the maximum margin to distinguish between positive and negative instances. Extended on the basis of multiple linear regression models, GLM can flexibly assess the relationship between normally distributed dependent features and categorical or continuously independent features. XGB, a collection of boosting trees based on gradient boosting, can be used for comparing between the classification error and the model complexity precisely. The "caret" R packages automatically adjusted the parameters in these models by grid search. All of these machine-learning models are executed with default parameters and evaluated by 5-fold cross-validation. The "DALEX" package was used for interpreting the above four machine learning models and visualizing residual distributions and feature importance among these machine learning models. In addition, the "pROC" R package (Ver. 1.18.0) was also executed to visualize the region under the ROC curve. Therefore, the best machine learning model was determined, and the top 5 important variables were considered as key predictor genes associated with sepsis.

Construction and Validation of a Nomogram Model

The "rms" R package was applied for establishing a nomogram model to evaluate the risk of pediatric sepsis. Each predictor has a corresponding score, and the "total score" represents the sum of the scores of each predictor. The predictive ability of the nomogram model was estimated through calibration curves, DCA and receiver operating characteristic (ROC).

Independent Validation Analysis

Two GSE13904 and GSE26440 datasets were used for validating the diagnose ability of 5 hub genes by the ROC analyses. ROC curves were visualized using the "pROC" R package. p value < 0.05 was considered as statistically significant.

Quantitative Real-Time PCR (qRT-PCR)

The whole blood samples of 25 pediatric sepsis and 14 healthy controls were collected from Women and Children's Hospital, School of Medicine, Xiamen University (Xiamen, China). The study received approval from the Ethics Committee of Women and Children's Hospital, Xiamen University (Number: KY-2021-035-K01), and written informed consents were obtained from the guardians of the pediatric participants. The screening criteria for sepsis patients were based on sepsis 3.0.[1] None of patients had a history of autoimmune disorders, neoplastic diseases, or oral immunosuppressants. Total RNA was extracted from whole blood using a RNAsimple total RNA kit (Tiangen, Beijing, China) and reverse-transcribed to cDNA using a FastKing RT kit (Tiangen, Beijing, China) according to the manufacturer's instructions. Quantitative Real-Time PCR was performed with a SYBR Green Master Mix (Tiangen, Beijing, China) according to the manufacturer's instructions. All primer sequences were shown in Table 1. Data were normalized to the GAPDH expression level of the internal reference control, and the relative expression levels of hub genes in different groups were calculated using $2^{-\Delta\Delta Ct}$ method.

Table 1 Primers for Quantitative Real-Time PCR

Gene	Primer	Sequence (5′–3′)
DHRS13	Forward	ATGTACTGTTTGCCCGGGAG
	Reverse	GGAACAGCTCCGAGTTCACA
CDA	Forward	CCGTCTCAGAAGGGTACAAG
	Reverse	GACAATATACGTACCATCCGG
GPR97	Forward	CAACACCTACTTCGGGCACT
	Reverse	AGAGGGCGTACATGGTTGTC
NQO2	Forward	TGGTCGGAAGATTGCTGGAC
	Reverse	ACCCTATCCATCCAGCCCTT
DYSF	Forward	GATGAGCCCAACATGAACCCTAAG
	Reverse	GGGAAGGCGTAGATGAAGATGG
GAPDH	Forward	GGTCTCCTCTGACTTCAACA
	Reverse	ATACCAGGAAATGAGCTTGA

Statistical Analysis

Statistical analysis was conducted using GraphPad Prism 8.0.1 software. Statistical significance was assessed using unpaired two-tailed Student's *t*-test with $p < 0.05$.

Results

Dysregulation of Pyroptosis-Related DEGs and Immune Infiltration in Pediatric Sepsis

To elucidate the potential roles of pyroptosis in pediatric sepsis, we first systematically analyzed the expression profiles of pyroptosis-related DEGs between septic children and normal controls based on GSE13904 dataset. The workflow diagram of this study was shown in Figure 1. We found a total of 32 pyroptosis-related DEGs (21 up-regulated and 11 down-regulated) (Figure 2A and B) and the locations of these DEGs were on the autosomes (Figure 2C). Subsequently, we conducted a correlation analysis to explore the interactive relationships of these pyroptosis-related DEGs, we found some pyroptosis-related DEGs, such as CHMP2A and PYCARD, showed a strong synergistic relationship (Figure 2D and E). Besides, we utilized CIBERSORT algorithm to evaluate the proportions of 22 infiltrated immune cell types in sepsis children and normal controls (Figure 2F), and the results revealed that the infiltration levels of naïve B cells, T regulatory

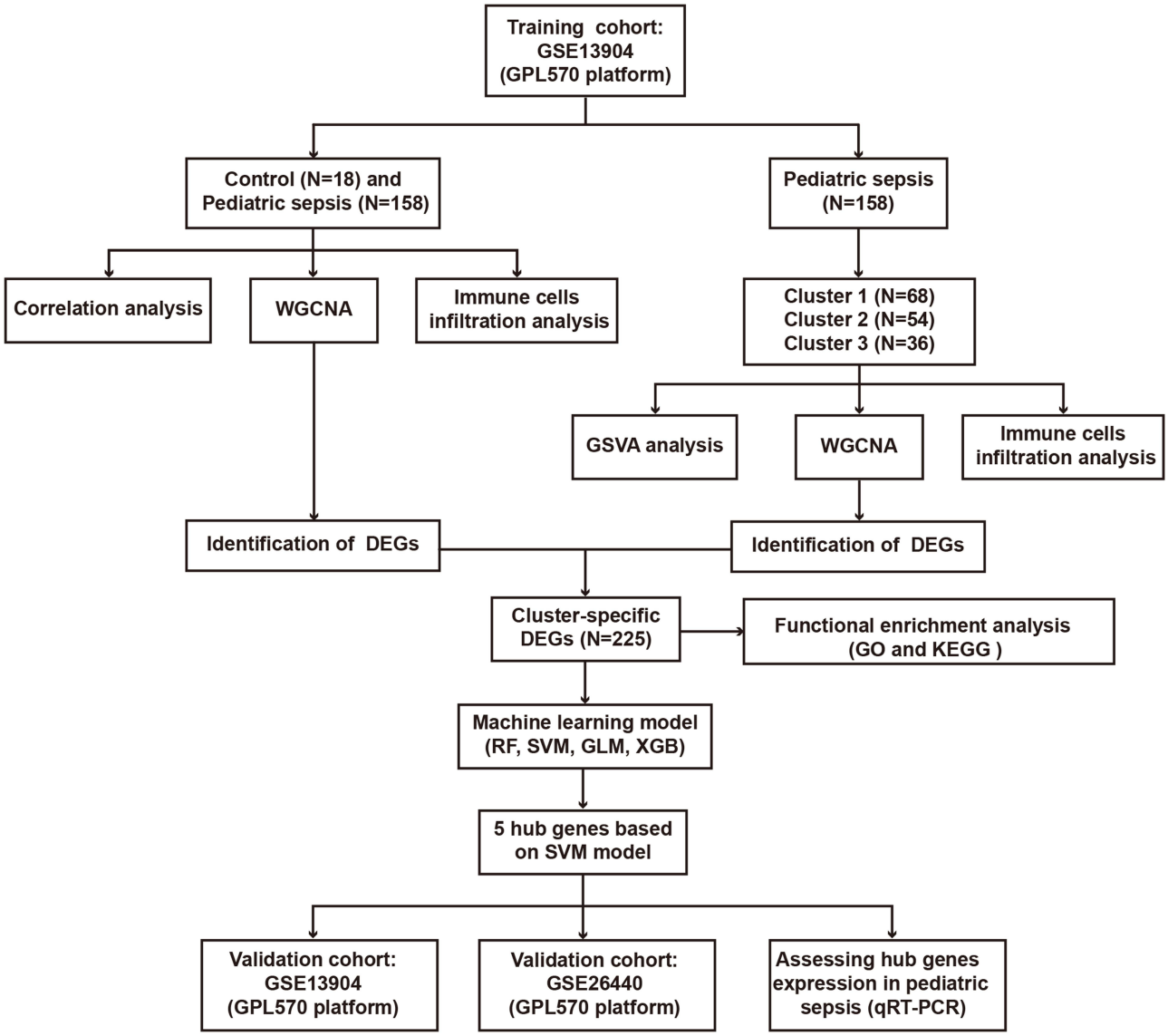

Figure 1 Workflow diagram of this study.

https://doi.org/10.2147/PHMT.S521939

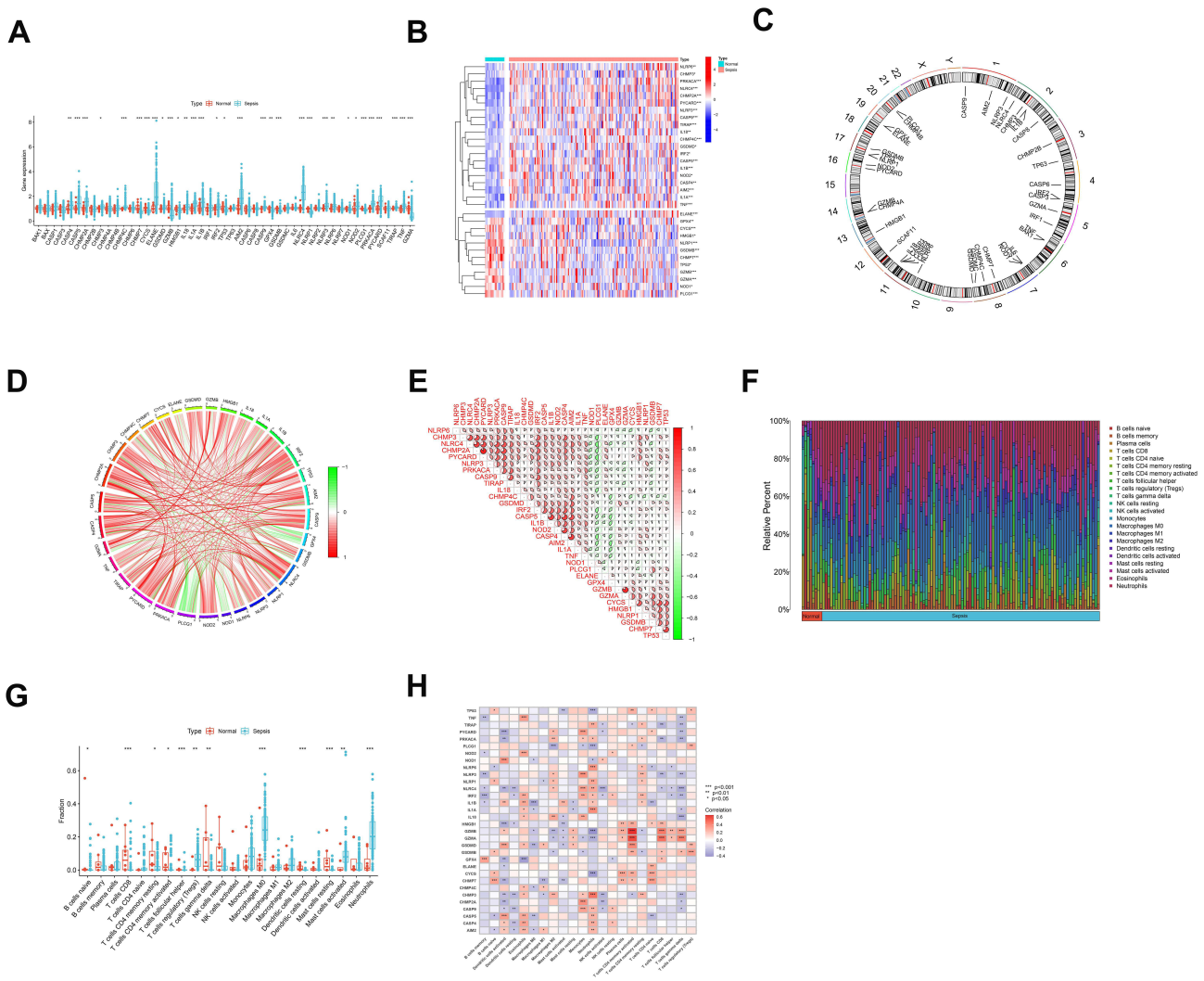

Figure 2 Identification of dysregulated pyroptosis-related DEGs and immune infiltration in pediatric sepsis. (**A** and **B**) Boxplots (**A**) and Heatmap (**B**) of the expression of 32 pyroptosis-related DEGs between pediatric sepsis and normal controls using "ggboxplot" and "pheatmap" packages based on R software (version 4.2.1). (**C**) The location of 32 pyroptosis-related DEGs on chromosomes. (**D** and **E**) Correlation network analysis of the pyroptosis-related DEGs. (**F**) The relative abundances of 22 infiltrated immune cells between pediatric sepsis and normal controls. (**G**) The differences in immune infiltration between pediatric sepsis and normal controls. (**H**) The correlation analysis between 32 pyroptosis-related DEGs and infiltrated immune cells. *$p < 0.05$, **$p < 0.01$, ***$p < 0.001$.

cells (Tregs), M0 macrophages, activated mast cells and neutrophils in sepsis children were significantly higher than normal controls (Figure 2G), suggesting that the variation of the immune system may be involved in the occurrence and pathological progression of pediatric sepsis. Meanwhile, correlation analysis between 32 pyroptosis-related DEGs and infiltrated immune cells indicated that activated memory $CD4^+$ T cells were strongly correlated with GZMB and GZMA (Figure 2H). These results revealed that pyroptosis-related DEGs may play a crucial role in the occurrence and progression of pediatric sepsis.

Identification of Pyroptosis-Related Molecular Clusters in Pediatric Sepsis

To further explore the pyroptosis-related expression patterns in pediatric sepsis, a total of 158 pediatric sepsis samples were clustered using a consistent clustering algorithm based on the pyroptosis-related DEGs expression profiles. According to the relative change in area under the CDF curves, k = 3 was determined to be the optimum point for cluster (Figure 3A–C). We finally divided 158 pediatric sepsis patients into three clusters, including cluster 1 (n = 68), cluster 2 (n = 54) and cluster 3 (n = 36) (Figure 3D). Finally, we assessed the expression differences of 32 DEGs among Cluster 1, Cluster 2 and Cluster 3. The distinct pyroptosis-related DEGs among three clusters were observed (Figure 3E).

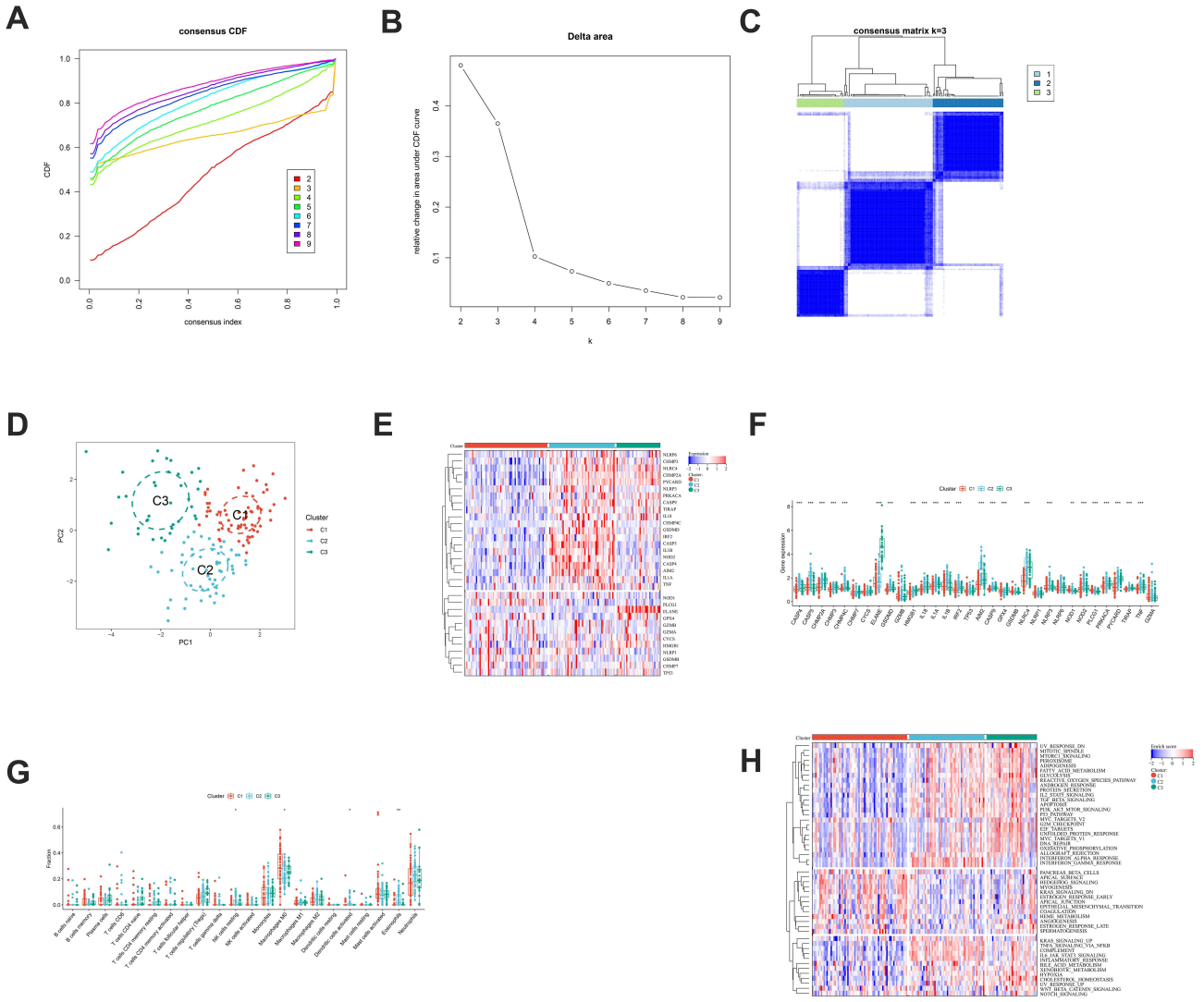

Figure 3 Identification of pyroptosis-related molecular clusters, immune infiltration characteristics and functional differences in pediatric sepsis. (**A**) CDF delta area curves. (**B**) The score of consensus clustering. (**C**) Consensus clustering matrix when k = 3. (**D**) PCA verified three patterns in in pediatric sepsis. (**E** and **F**) The pyroptosis-related genes expression in the three clusters. (**G**) The differences in immune infiltration in pyroptosis-related molecular clusters. (**H**) The functional differences in pyroptosis-related molecular clusters. *$p < 0.05$, **$p < 0.01$ ***$p < 0.001$.

The results revealed that CHMP2A, ELANE, HMGB1, GPX4, NLRP1 and PYCARD were highly expressed in cluster 3, while CASP4, CASP5, CHMP3, CHMP4C, GSPMD, IL-18, IL-1A, IL-1B, IRF2, AIM2, CASP9, NLRP3, NOD2, PRKACA, TIRAP and TNF were enhanced in cluster 2. Besides, only two genes NOD1 and PLCG1were upregulated in cluster 1 (Figure 3F).

Evaluating the Immune Infiltration Characteristics and Functional Differences in Three Clusters

Next, we analyzed the immune cell infiltration to evaluate the immunological features of different pyroptosis-related clusters. The results shown the levels of resting NK cells, activated dendritic cells and eosinophils were upregulate in cluster 2, whereas the levels of M0 macrophages were relatively higher in cluster 1 (Figure 3G). To further interpret the functional differences in three distinct pyroptosis-related clusters, GSVA was performed. The GSVA revealed that MTORC1 signaling, glycolysis, IL2-STAT5 signaling, TGF-beta signaling, apoptosis, PI3K-AKT-MTOR signaling, TP53 pathway, KRAS signaling and inflammatory response were reinforced in cluster 3 and cluster 2, while hedgehog signaling, KRAS signaling and epithelial-mesenchymal transition were upregulated in cluster1 (Figure 3H).

https://doi.org/10.2147/PHMT.S521939

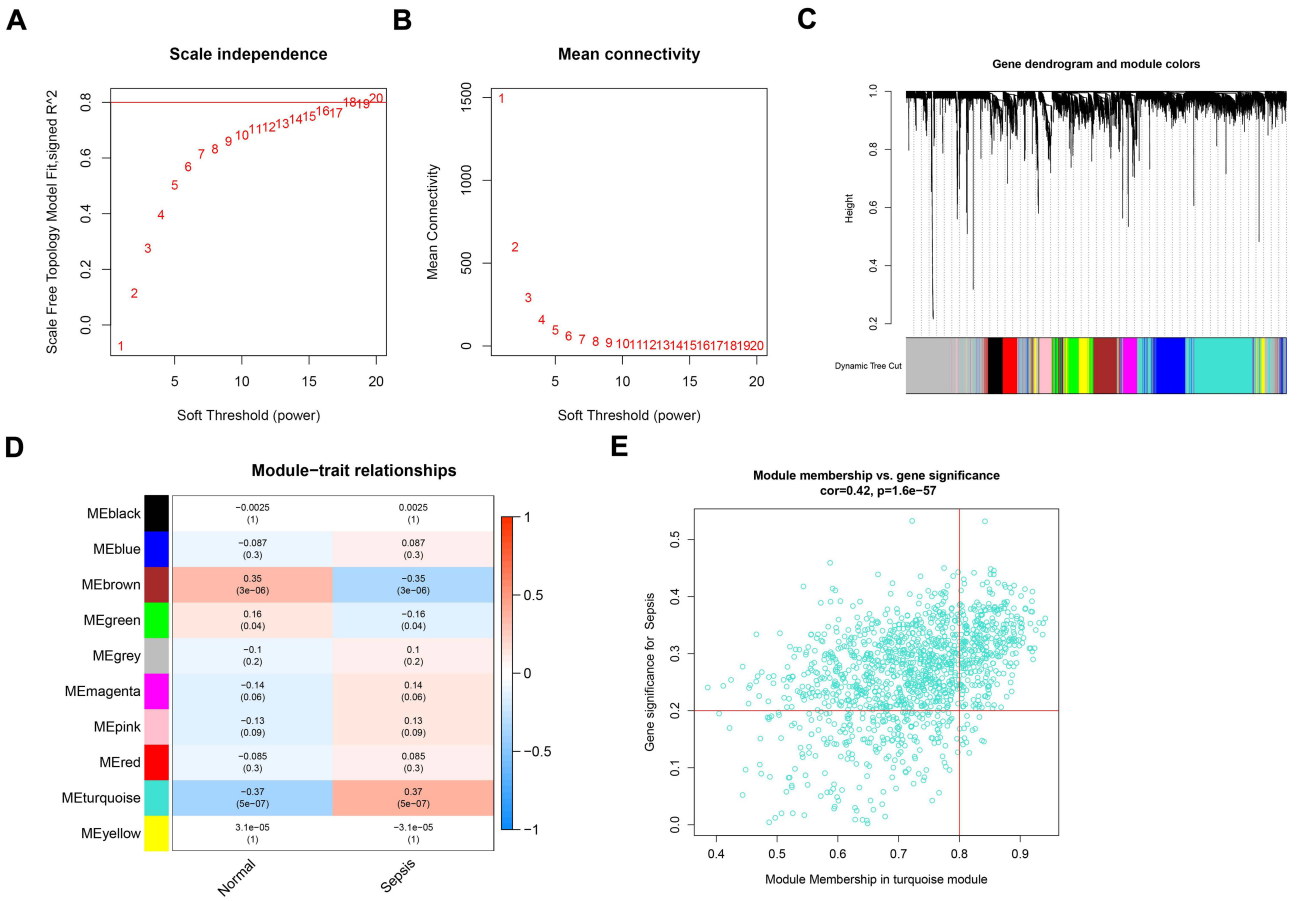

Figure 4 Co-expression network of pyroptosis-related DEGs in pediatric sepsis. (**A** and **B**) The selection of soft threshold power. (**C**) Cluster tree dendrogram of co-expression modules. (**D**) Correlation analysis between module characteristics and clinical status. (**E**) Scatter plot between module membership in turquoise module and the gene significance for pediatric sepsis.

Gene Modules Screening and Co-Expression Network Construction

To identify the key gene modules associated with pediatric sepsis, we established co-expression networks and modules for pediatric sepsis and normal controls using the WGCNA algorithm. We calculated the variance of each gene expression in GSE13904, and then selected the top 25% genes with the large variance for further analysis. Co-expressed gene modules were established when the value of soft power was selected to 18 and the scale-free $R^2 = 0.8$ (Figure 4A and 4B). Using the dynamic cutting algorithm, we obtained 10 different co-expression modules with different colors (Figure 4C). Then these genes in 10 color modules were consecutively applied to analyze the similarity and adjacency of the clinical features of the modules, and the turquoise module has the strongest relationship with pediatric sepsis (Figure 4D). Finally, we found a positive correlation between turquoise modules and module-related genes, including 325 genes closely related to pediatric sepsis (Figure 4E).

We also used the WGCNA algorithm to analyze the key gene modules closely related to pyroptosis-related clusters. We screened $\beta = 17$ and $R^2 = 0.7$ as the most appropriate soft threshold parameters for establishing a scale-free network (Figure 5A and B). A total of 10 different co-expression modules with different colors were acquired using the dynamic cutting algorithm (Figure 5C). There was a high correlation between the blue module and pediatric sepsis through module-clinical features relationship analysis (Figure 5D). Moreover, the blue module genes had a positive relationship with the blue module through the correlation analysis (Figure 5E).

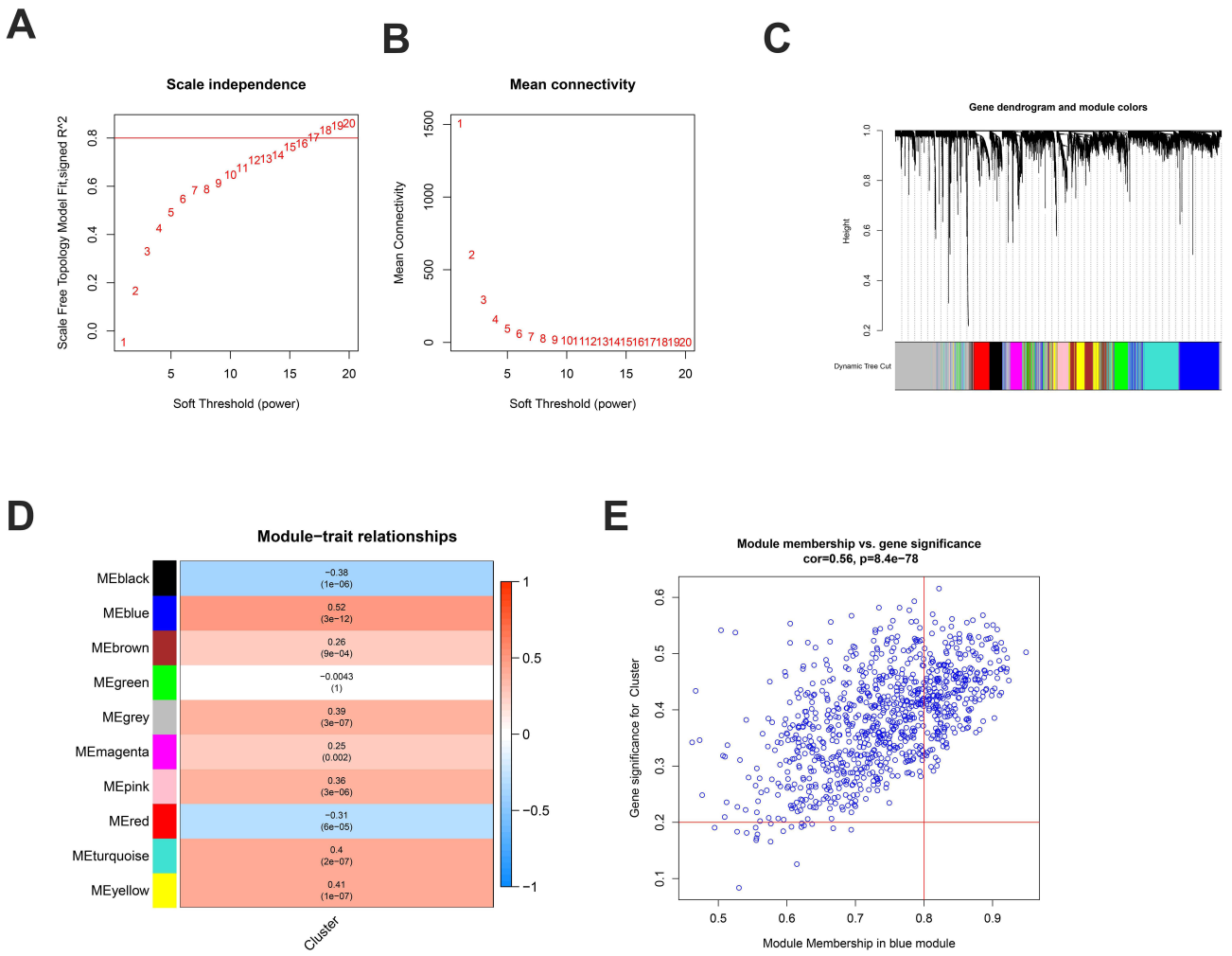

Figure 5 Co-expression network of pyroptosis-related DEGs in the three clusters. (**A** and **B**) The selection of soft threshold power. (**C**) Cluster tree dendrogram of co-expression modules. (**D**) Correlation analysis between module characteristics and clinical status. (**E**) Scatter plot between module membership in turquoise module and the gene significance for cluster.

Identification and Functional Enrichment Analysis of Cluster-Specific DEGs

In order to identify cluster-specific DEGs, we analyzed the intersections between module-related genes of normal and septic children and module-related genes of pyroptosis clusters, and obtained a total of 225 cluster-specific DEGs (Figure 6A). GO and KEGG enrichment analysis were conducted to further analyze the possible biological functions of these 225 cluster-specific DEGs. In the GO-BP analysis, the cluster-specific DEGs were primarily associated with cell activation in immune respond, including leukocyte activation, myeloid leukocyte activation, and neutrophil activation, ect (Figure 6B). In the GO-CC analysis, the main cluster-specific DEGs were enriched in the cytoplasmic vesicle and intracellular vesicle (Figure 6C). In the GO-MF analysis, most of the cluster-specific DEGs were enriched in the enzyme binding and identical protein binding (Figure 6D). In addition, KEGG pathway analysis indicated the cluster-specific DEGs were relevant to the chemokine signaling pathway and B cell receptor signaling pathway (Figure 6E).

Construction and Evaluation of Machine Learning Models

In order to further identify the intersection genes with potential diagnostic value, we utilized four validated machine learning models, including RF, SVM, GLM, and XGB, based on the expression profiles of 225 cluster-specific DEGs. The "DALEX" package was used to interpret the four models and plot the residual distribution for each model in the test set. And the results shown that RF and SVM had relatively lower residuals (Figure 7A and B). Subsequently, the top 10 important characteristic

https://doi.org/10.2147/PHMT.S521939

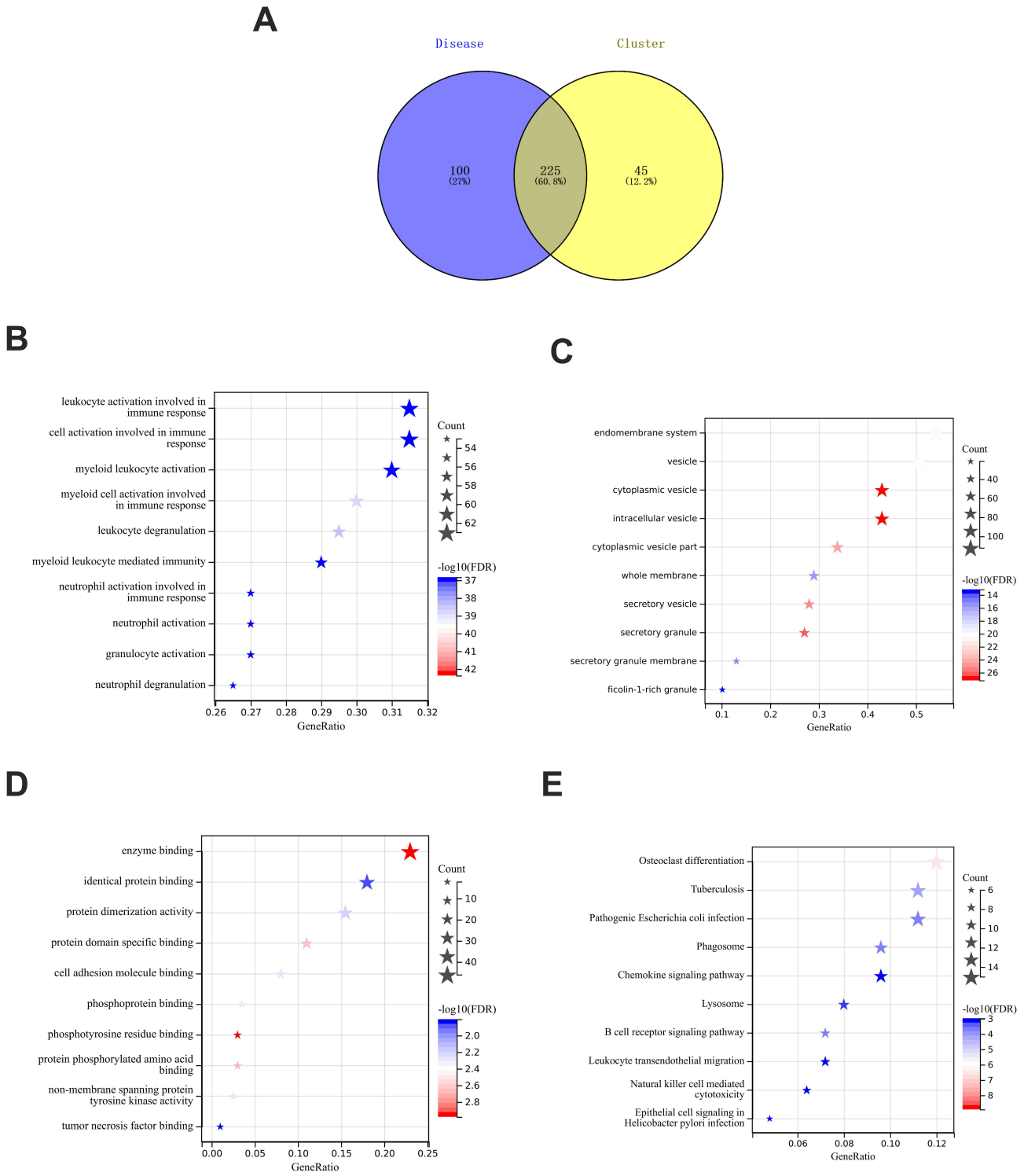

Figure 6 Identification and functional enrichment analysis of cluster-specific DEGs. (**A**) The intersections between module-related genes in the GSE13904 cohort and module-related genes of pyroptosis clusters. (**B**–**E**) GO and KEGG pathway enrichment analysis of the cluster-specific DEGs.

variables of each model were ranked based on the root mean square error (RMSE) (Figure 7C). In addition, the diagnostic performance of the four machine learning algorithms was evaluated by using ROC according to 5-fold cross-validation. The SVM model exhibited maximum area under the ROC curve (AUC) (GLM, AUC = 0.545; SVM, AUC = 0.991; RF, AUC =

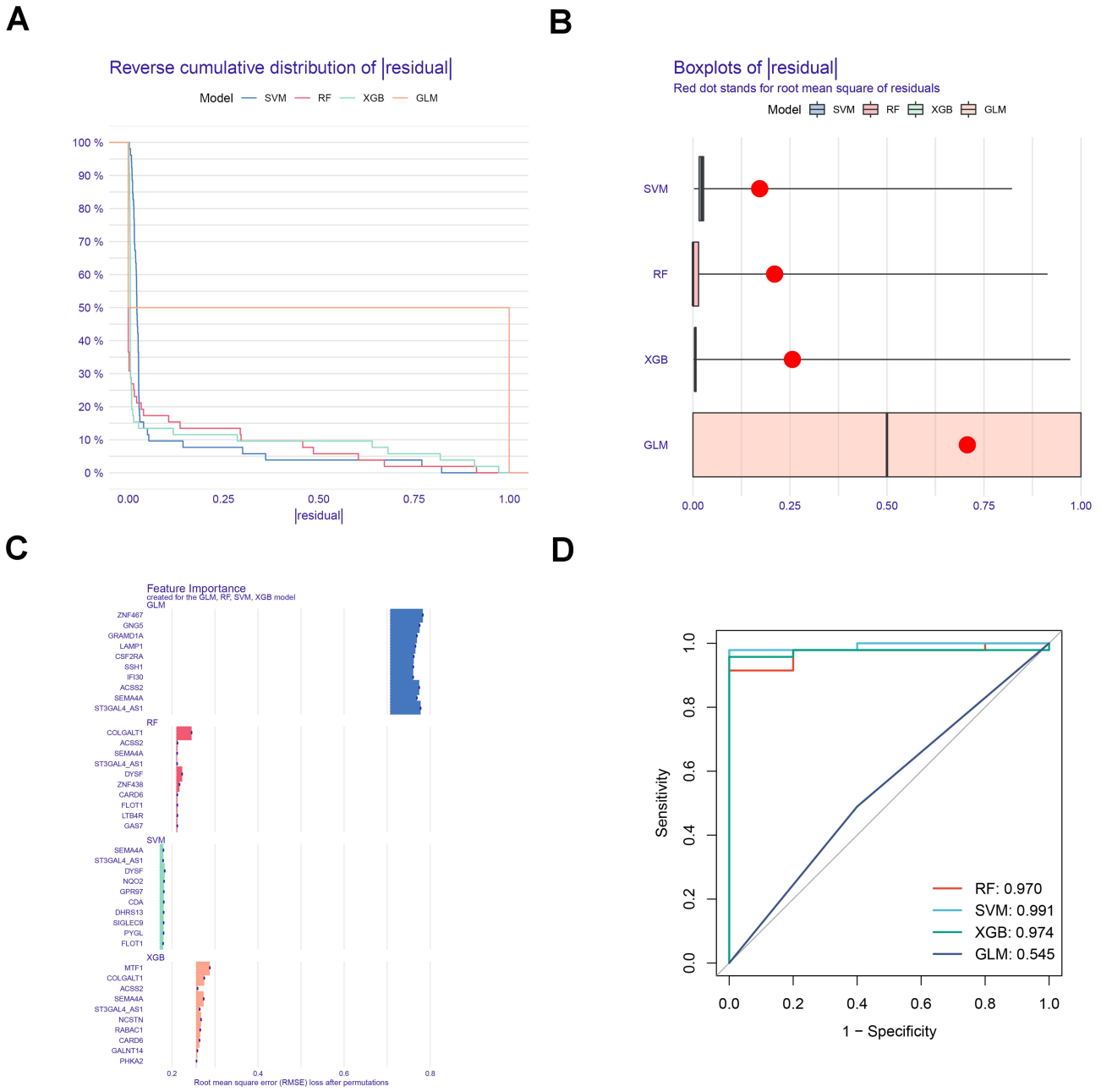

Figure 7 Construction and evaluation of RF, SVM, GLM and XGB machine models. (**A**) Cumulative residual distribution of each machine learning model. (**B**) The residuals of each machine learning model. (**C**) The important genes in RF, SVM, GLM and XGB machine models. (**D**) ROC analysis of four machine learning models based on 5-fold cross-validation.

0.970; XGB, AUC = 0.974; Figure 7D). Overall, these results indicated the SVM model was the optimal model to predict pediatric sepsis.

The top five important hub genes in SVM model (DHRS13, CDA, GPR97, NQO2 and DYSF) were selected for further analysis. A nomogram was first constructed to evaluate the risk of sepsis children (Figure 8A). Calibration curve and DCA were used to evaluate the predictive efficiency of the nomogram model. The deviation between the actual clusters risk and the predicted risk was very small by analyzing the calibration curve (Figure 8B). Meanwhile, the DCA also showed that the nomogram has a high accuracy, which may provide a basis for clinical decision making (Figure 8C). Subsequently, we verified the predictive model of the 5 hub genes on the external GSE26440 dataset. The ROC curve showed that the

https://doi.org/10.2147/PHMT.S521939

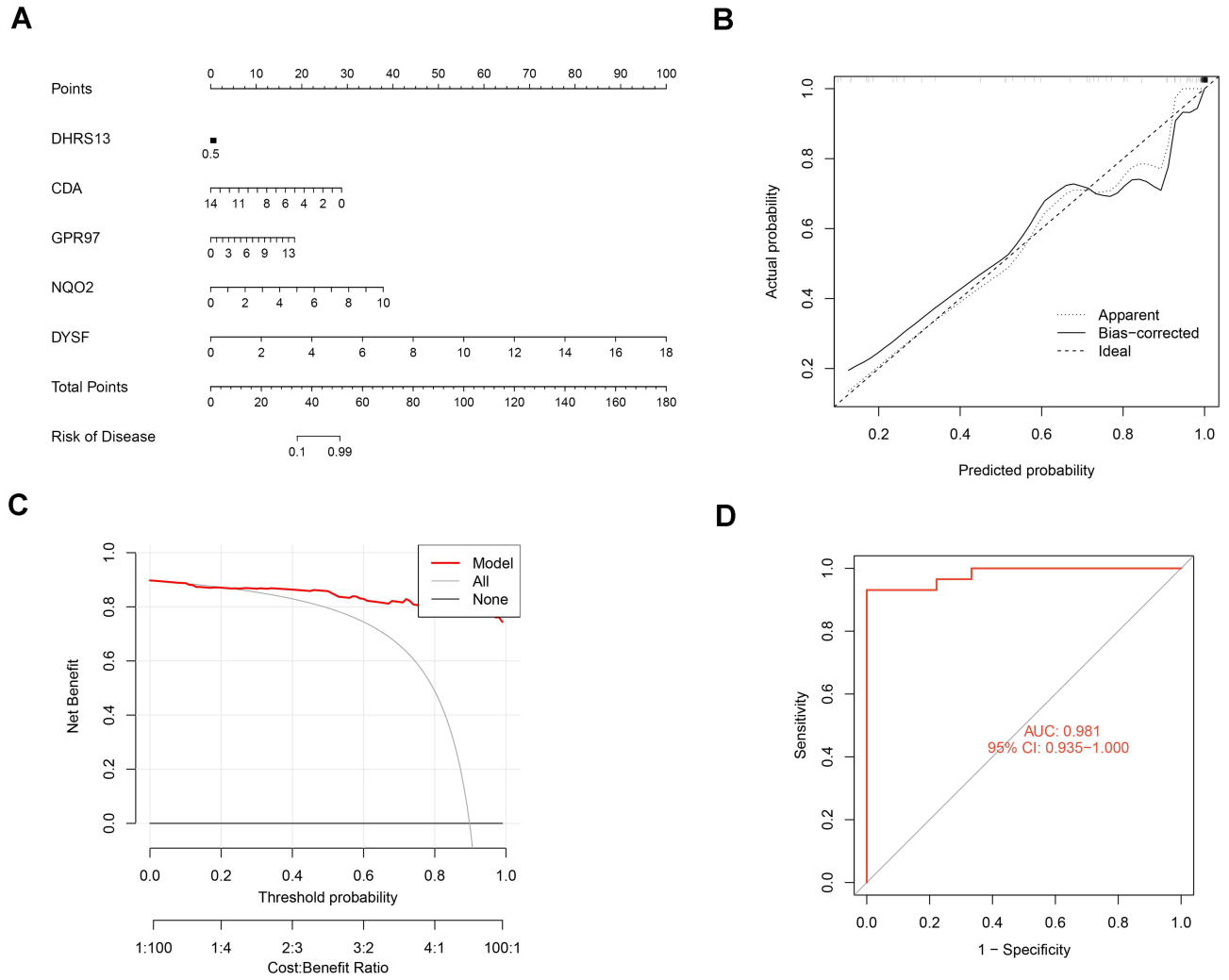

Figure 8 Validation of the 5 hub genes based on SVM model. (**A**) Construction of a nomogram for predicting the risk of pediatric sepsis. (**B**) Construction of calibration curve. (**C**) The decision curve analysis (DCA). (**D**) ROC analysis of the 5-gene-based SVM model based on 5-fold cross-validation.

predictive performance of the 5 hub genes was satisfactory and the AUC value was 0.981, which indicated that our predictive model was equally effective in distinguishing sepsis children from normal individuals (Figure 8D).

Diagnostic Performance of 5 Hub Genes in Pediatric Sepsis

Then, we verified the expression and diagnostic performance of the 5 hub genes in the GSE13904 and GSE26440 datasets. The results indicated that compared with normal control children, the 5 hub genes were upregulated in pediatric sepsis in GSE13904 and GSE26440 datasets (Figure 9A and B). Besides, the ROC curve analysis showed that 5 hub genes had a high diagnostic performance in GSE13904 and GSE26440 datasets (Figure 9C and D). Combined with these results, the 5 hub genes may be used as diagnostic biomarkers for pediatric sepsis.

Expression Validation of Hub Genes in Whole Blood From Pediatric Sepsis

Finally, qRT-PCR was used to verify the expression levels of 5 hub genes in whole blood between the pediatric sepsis group and the control group. The results were consistent with those of the bioinformatics analysis, which showed significantly enhanced expression levels of five genes (DHRS13, CDA, GPR97, NQO2 and DYSF) in the pediatric sepsis group compared to the healthy control group (Figure 10A–E).

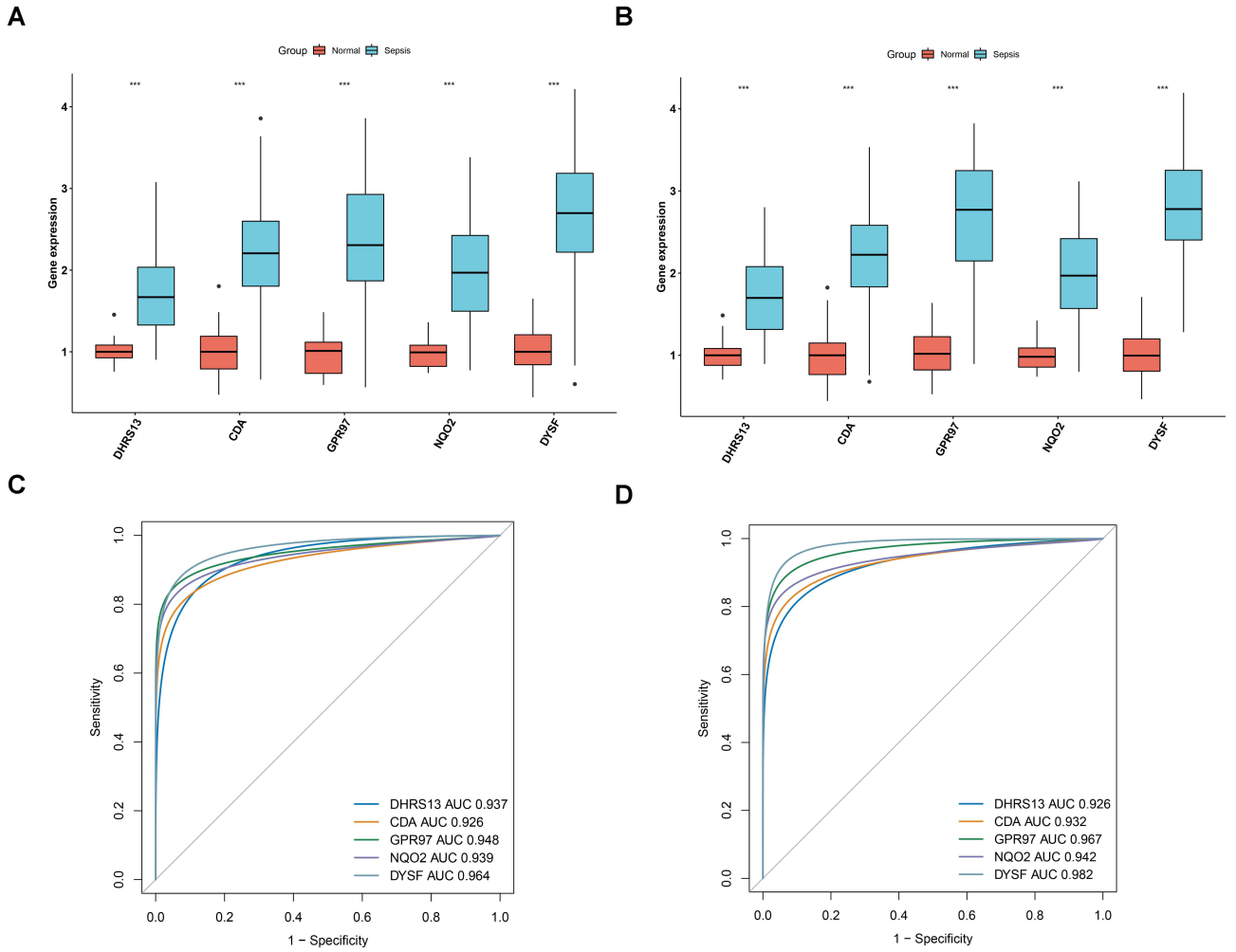

Figure 9 The performance of 5 hub genes to diagnose pediatric sepsis in the GSE13904 and GSE26440 datasets. (**A**) Expression differences of 5 hub genes in the pediatric sepsis and control groups in GSE13904 database. (**B**) Expression differences of 5 hub genes in the pediatric sepsis and control groups in GSE26440 database. (**C**) The ROC curve of the 5 hub gene in GSE13904 database. (**D**) The ROC curve of the 5 hub gene in GSE26440 database. ***$p < 0.001$.

Discussion

Sepsis is an extremely complex process involving a series of inflammatory and anti-inflammatory processes, humoral and cellular responses, and circulatory disorders.[24] Despite progress in care and treatment, sepsis remains the leading cause of death of pediatric deaths worldwide, and the clinical presentation of pediatric sepsis may be subtle and difficult to identify.[25] In order to establish an early diagnosis and a personalized treatment strategy, clinicians are in need of reliable biomarkers for pediatric sepsis. Recently, Studies have demonstrated that pyroptosis is involved in the regulation of inflammation and immune responses, suggesting that pyroptosis plays an essential role in in sepsis.[19] However, the regulatory roles and potential mechanisms of pyroptosis in pediatric sepsis have not been fully revealed. Therefore, we attempted to elucidate the specific role of pyroptosis-related DEGs and the immune microenvironment in pediatric sepsis.

In this study, we first analyzed the expression profiles of pyroptosis-related DEGs in septic children and healthy controls. The results indicated that expression levels of pyroptosis-related DEGs were dysregulated in septic children, suggesting a pivotal role of pyroptosis-related DEGs in the occurrence and development of septic children. Subsequently, we calculated the correlation among pyroptosis-related DEGs to elucidate the relationship between pyroptosis and pediatric sepsis. We discovered that most pyroptosis-related DEGs presented significant synergistic, which revealed the interactions of pyroptosis-related DEGs have a specific impact on septic children. Next, through CIBERSORT algorithm to analysis of immune cell infiltration, we found that septic children presented higher infiltration levels of naïve

https://doi.org/10.2147/PHMT.S521939

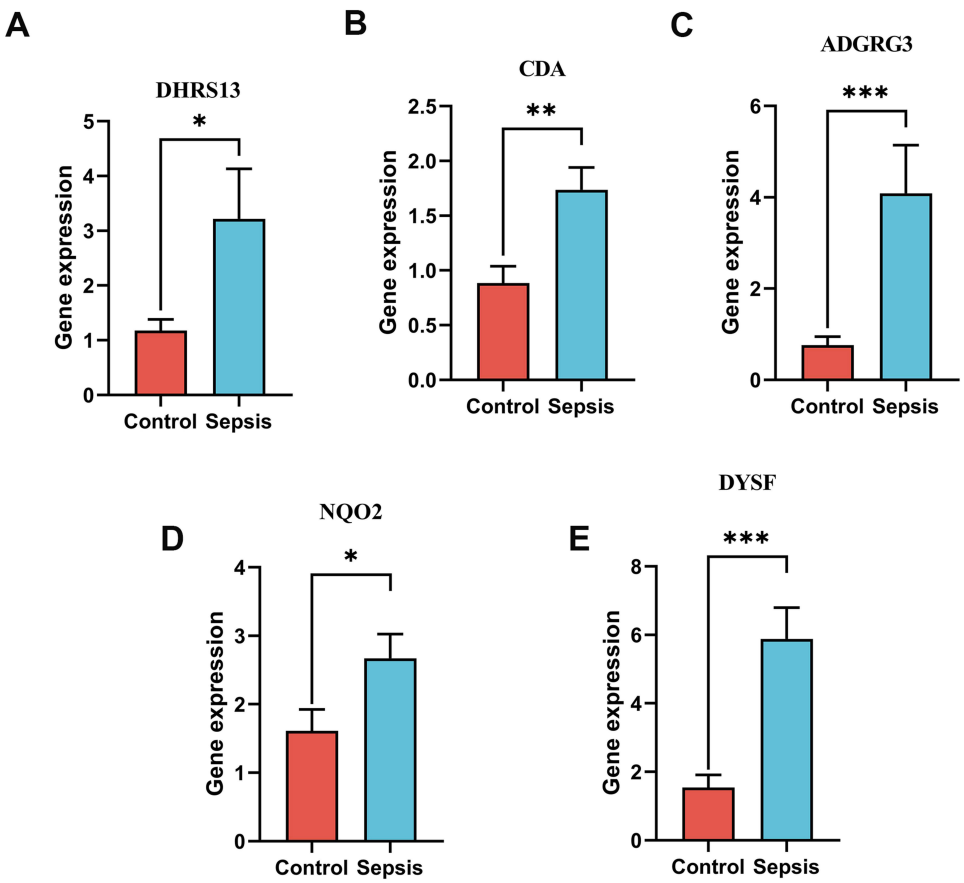

Figure 10 Hub genes expression in whole blood from sepsis patients and healthy controls. (**A**) DHRS13. (**B**) CDA. (**C**) GPR97. (**D**) NQO2. (**E**) DYSF. *$p < 0.05$, **$p < 0.01$ ***$p < 0.001$.

B cells, T regulatory cells (Tregs), M0 macrophages, activated mast cells and neutrophils. Recent studies have shown that immune cells play key roles in the maintenance of peripheral homeostasis and immune regulation in sepsis.[26] The pathophysiology of sepsis is considered to be characterized by an initial uncontrolled inflammatory response followed by an immunosuppressive phase. And the immune cells (such as neutrophils, macrophages, Tregs, DCs and NK cells) can not only trigger inflammatory events by producing inflammatory cytokines, but also induce extensive lymphocyte apoptosis. The apoptotic depletion of immune cells and increased Treg expression are involved in sepsis-induced immunosuppression.[27,28] Besides, we used unsupervised cluster analysis to elucidate the different pyroptosis patterns in septic children based on the expression profiles of pyroptosis-related DEGs, and three distinct pyroptosis-relate clusters were identified. The proportions of resting NK cells, M0 macrophages and activated dendritic cells in three clusters were significantly different, suggesting the crucial role of these immune cells in pediatric sepsis. Meanwhile, Cluster 1 was mainly enriched in KRAS signaling; Cluster 2 was related to inflammatory response, TNF-α and TNF-β response; Cluster 3 was characterized by mitotic spindle, TGF-β signaling and apoptosis etc. It was reported that TGF-β plays a key role in the severe septic inflammatory responses including high permeability, increased expressions of inflammatory-related genes.[29] Besides, cell apoptosis, especially immune cell apoptosis, is closely significantly correlated with poor outcomes of the septic patients.[30] Finally, the functions of cluster-specific DEGs mainly focused on immune cell activation, further suggesting that the crucial role of immune cell in pediatric sepsis.

Recently, multiple machine learning methods have been widely used to predict diseases prevalence.[31] It is known that multifactorial analyses have a lower error rate and more reliable results compared to univariate analysis. In this study, we analyzed the predictive performance of the machine learning models (RF, SVM, GLM, and XGB) based on the expression profiles of cluster-specific DEGs and constructed an SVM-based prediction model. The SVM-

based prediction model has the highest predictive efficacy in the testing cohort (AUC = 0.991), suggesting the SVM-based machine learning has satisfactory performance in predicting the subtypes of pediatric sepsis. SVM outperformed other algorithms. This advantage likely stems from the highly nonlinear and complex nature of sepsis data, where multiple immune interactions create intricate patterns that linear models fail to capture. SVM's use of kernel functions, particularly the radial basis function (RBF) kernel, enables effective mapping into higher-dimensional spaces to identify optimal separating hyperplanes, thereby improving classification accuracy and generalization. Furthermore, SVM is well-suited for high-dimensional, small-sample datasets by maximizing the margin and reducing overfitting risk. Subsequently, we selected five important hub genes (DHRS13, CDA, GPR97, NQO2 and DYSF) to construct a 5-gene-based SVM model. Meanwhile, we used qRT-PCR to verify the expression levels of five hub genes in whole blood from clinical samples. The results showed increased expression levels of the five genes in the pediatric sepsis group compared to the healthy control, which is consistent with our bioinformatics results. Dehydrogenase/reductase 13 (DHRS13) is one of the short-chain dehydrogenase/reductase (SDR) superfamily numbers,[32] and it can be served as a novel biomarker for prediction of hepatocellular carcinoma, acute myocardial infarction (AMI) and the outcomes of $HER2^{+}$ breast cancer after neoadjuvant chemotherapy.[33–35] However, the functions of DHRS13 in sepsis are unclear. Cytidine deaminase (CDA) is a ubiquitous enzyme that is mainly involved in free pyrimidine recycling,[36] which catalyzes the hydrolytic deamination of cytidine and deoxycytidine (DC) to uridine and deoxyuridine.[37] Studies have indicated that CDA is closely associated with rheumatoid arthritis, systemic lupus erythematosus and pre-eclampsia.[38–40] Arne Bøyum et al's research indicated that CDA was up-regulated in patients with different clinical presentations of meningococcal infection, and the highest levels were detected in nonsurviving patients with persistent septic shock.[41] However, few researches have focused on the function of CDA in sepsis, which is worth further study. GPR97 is a type of adhesion G protein-coupled receptors (GPCRs),[20] which is expressed on leukocytes, such as neutrophils, eosinophils, and mast cells.[21] GPR97 has been reported to play an integral role in the regulation of B cell fate, especially CREB and NF-κB signaling pathways.[22] Taken together, GPR97 may be participated in immunological disorders, such as sepsis. Quinone oxidoreductase 2 (NQO2) is flavoproteins, which can oxidize a variety of analogues of dihydronicotinamide. Recent studies have revealed that NQO2 is involved in initiation and progression of tumors probably via the production of reactive oxygen species (ROS) during quinone metabolism.[23] ROS can regulate immune signals, which results in affecting the pathogenesis of sepsis and causing damage to cells and organs.[42] Thus, NQO2 may be involved in the development of sepsis by regulating ROS. Dysferlin (DYSF) is a type II transmembrane protein, which is involved in the muscle membrane repair and the regulation of cell adhesion in human monocytes. Zhenjiang Bai et al found the DYSF expression levels in the sepsis group were significantly higher than those of the control group based on a comprehensive microarray analysis,[43] which further illustrates the value of DYSF in pediatric sepsis. The 5-gene-based SVM model presents a satisfactory predictive ability in pediatric sepsis (AUC = 0.981), which provides new insights into the diagnosis of pediatric sepsis. Besides, the five genes in early diagnosis of pediatric sepsis were remarkable in both training and validation sets by ROC analysis, further suggesting the predictive efficacy of these five genes. Taken together, the 5-gene-based SVM model is a satisfactory indicator for predicting pediatric sepsis.

There are still some limitations in this study. First, the primary analyses were based on retrospective data from public databases, which may introduce selection bias and limit the generalizability of the findings. Second, the qRT-PCR validation was conducted in a relatively small cohort, which may not fully capture the heterogeneity of pediatric sepsis. Further validation in larger, prospective clinical cohorts is warranted. In addition, the current study focused primarily on computational and expression-level analyses without direct functional validation of the identified genes. To address this, future studies will incorporate in vivo and in vitro models—such as gene knockout or overexpression systems — to elucidate the mechanistic roles of key pyroptosis-related genes in pediatric sepsis. These approaches will help clarify causal relationships and support the development of targeted therapeutic strategies.

Conclusions

In conclusion, we identified pyroptosis-related molecular clusters and immune infiltration characterization in pediatric sepsis. And we constructed a 5-gene-based SVM model as a promising predictive model and identified five hub genes (DHRS13, CDA, GPR97, NQO2 and DYSF) as diagnostic markers for pediatric sepsis. The results of this study can provide new insights for pyroptosis in pediatric sepsis and facilitate the development of novel biomarkers for pediatric sepsis. However, given the limited sample size and retrospective nature of the data, these results should be interpreted with caution. Future multicenter prospective studies are warranted to validate the robustness and clinical applicability of our model.

Data Sharing Statement

The datasets presented in this study can be found the Gene Expression Omnibus (GEO) website (https://www.ncbi.nlm.nih.gov/geo), with the following data accession identifiers: GSE13904 and GSE26440.

Ethics Statement

This study was approved by the Ethics Committee of Women and Children's Hospital, Xiamen University (Number: KY-2023-074-H01). All patients provided signed informed consent.

Acknowledgment

We sincerely thank all who participated in this study.

Author Contributions

All authors made a significant contribution to the work reported, whether that is in the conception, study design, execution, acquisition of data, analysis and interpretation, or in all these areas; took part in drafting, revising or critically reviewing the article; gave final approval of the version to be published; have agreed on the journal to which the article has been submitted; and agree to be accountable for all aspects of the work.

Funding

This work was sponsored by Fujian Provincial Health Technology Project (grant number 2020QNB069), Xiamen Medical and Health Guidance Project (grant number 3502Z20214ZD1229), Major Science and Technology Project of Fujian Provincial Health Commission (2021ZD01006, founded by Xiamen Municipal Health Commission).

Disclosure

The authors declare that the research was conducted in the absence of any commercial or financial relationships that could be construed as a potential conflict of interest.

References

1. Singer M, Deutschman CS, Seymour CW, et al. The Third International Consensus Definitions for Sepsis and Septic Shock (Sepsis-3). *JAMA*. 2016;315(8):801–810. doi:10.1001/jama.2016.0287
2. Yuniar I, Hafifah CN, Adilla SF, et al. Prognostic factors and models to predict pediatric sepsis mortality: a scoping review. *Front Pediatr*. 2022;10:1022110. doi:10.3389/fped.2022.1022110
3. Luxen M, van Meurs M, Molema G. Unlocking the Untapped Potential of Endothelial Kinase and Phosphatase Involvement in Sepsis for Drug Treatment Design. *Front Immunol*. 2022;13:867625. doi:10.3389/fimmu.2022.867625
4. Rudd KE, Johnson SC, Agesa KM, et al. Global, regional, and national sepsis incidence and mortality, 1990-2017: analysis for the Global Burden of Disease Study. *Lancet*. 2020;395(10219):200–211. doi:10.1016/S0140-6736(19)32989-7
5. Sanyaolu A, Patidar R, Ayodele O, Marinkovic A, Desai P. Pediatric Sepsis: the Importance of Understanding Criteria for Diagnosis. *Pediatr Ann*. 2022;51(10):e405–e408. doi:10.3928/19382359-20220803-07
6. Downes KJ, Fitzgerald JC, Weiss SL. Utility of Procalcitonin as a Biomarker for Sepsis in Children. *J Clin Microbiol*. 2020;58(7). doi:10.1128/JCM.01851-19
7. Wong HR. Pediatric sepsis biomarkers for prognostic and predictive enrichment. *Pediatr Res*. 2022;91(2):283–288. doi:10.1038/s41390-021-01620-5
8. Caraballo C, Jaimes F. Organ Dysfunction in Sepsis: an Ominous Trajectory From Infection To Death. *Yale J Biol Med*. 2019;92(4):629–640.
9. Wang X, Guo Z, Wang Z, et al. Diagnostic and predictive values of pyroptosis-related genes in sepsis. *Front Immunol*. 2023;14:1105399. doi:10.3389/fimmu.2023.1105399

10. Rao Z, Zhu Y, Yang P, et al. Pyroptosis in inflammatory diseases and cancer. *Theranostics*. 2022;12(9):4310–4329. doi:10.7150/thno.71086
11. Bergsbaken T, Fink SL, Cookson BT. Pyroptosis: host cell death and inflammation. *Nat Rev Microbiol*. 2009;7(2):99–109. doi:10.1038/nrmicro2070
12. Wu Y, Zhang J, Yu S, et al. Cell pyroptosis in health and inflammatory diseases. *Cell Death Discov*. 2022;8(1):191. doi:10.1038/s41420-022-00998-3
13. Zheng X, Chen W, Gong F, Chen Y, Chen E. The Role and Mechanism of Pyroptosis and Potential Therapeutic Targets in Sepsis: a Review. *Front Immunol*. 2021;12:711939. doi:10.3389/fimmu.2021.711939
14. Song F, Hou J, Chen Z, et al. Sphingosine-1-phosphate Receptor 2 Signaling Promotes Caspase-11-dependent Macrophage Pyroptosis and Worsens Escherichia coli Sepsis Outcome. *Anesthesiology*. 2018;129(2):311–320. doi:10.1097/ALN.0000000000002196
15. Yang D, He Y, Munoz-Planillo R, Liu Q, Nunez G. Caspase-11 Requires the Pannexin-1 Channel and the Purinergic P2X7 Pore to Mediate Pyroptosis and Endotoxic Shock. *Immunity*. 2015;43(5):923–932. doi:10.1016/j.immuni.2015.10.009
16. Liu L, Sun B. Neutrophil pyroptosis: new perspectives on sepsis. *Cell Mol Life Sci*. 2019;76(11):2031–2042. doi:10.1007/s00018-019-03060-1
17. Xi X, Zhang R, Chi Y, Zhu Z, Sun R, Gong W. TXNIP Regulates NLRP3 Inflammasome-Induced Pyroptosis Related to Aging via cAMP/PKA and PI3K/Akt Signaling Pathways. *Mol Neurobiol*. 2024;61(10):8051–8068. doi:10.1007/s12035-024-04089-5
18. Zhou C, Guo Q, Lin J, et al. Single-Cell Atlas of Human Ovaries Reveals The Role Of The Pyroptotic Macrophage in Ovarian Aging. *Adv Sci*. 2024;11(4):e2305175. doi:10.1002/advs.202305175
19. Wen R, Liu YP, Tong XX, Zhang TN, Yang N. Molecular mechanisms and functions of pyroptosis in sepsis and sepsis-associated organ dysfunction. *Front Cell Infect Microbiol*. 2022;12:962139. doi:10.3389/fcimb.2022.962139
20. Lin HH, Hsiao CC, Pabst C, Hebert J, Schoneberg T, Hamann J. Adhesion GPCRs in Regulating Immune Responses and Inflammation. *Adv Immunol*. 2017;136:163–201.
21. Peng YM, van de Garde MD, Cheng KF, et al. Specific expression of GPR56 by human cytotoxic lymphocytes. *J Leukocyte Biol*. 2011;90(4):735–740. doi:10.1189/jlb.0211092
22. Wang JJ, Zhang LL, Zhang HX, et al. Gpr97 is essential for the follicular versus marginal zone B-lymphocyte fate decision. *Cell Death Dis*. 2013;4(10):e853. doi:10.1038/cddis.2013.346
23. Hussein B, Ikhmais B, Kadirvel M, et al. Discovery of potent 4-aminoquinoline hydrazone inhibitors of NRH: quinoneoxidoreductase-2 (NQO2). *Eur J Med Chem*. 2019;182:111649. doi:10.1016/j.ejmech.2019.111649
24. Pierrakos C, Vincent JL. Sepsis biomarkers: a review. *Critical Care*. 2010;14(1):R15. doi:10.1186/cc8872
25. Emr BM, Alcamo AM, Carcillo JA, Aneja RK, Mollen KP. Pediatric Sepsis Update: how Are Children Different? *Surg Infect*. 2018;19(2):176–183. doi:10.1089/sur.2017.316
26. Rimmele T, Payen D, Cantaluppi V, et al. Immune Cell Phenotype and Function in Sepsis. *Shock*. 2016;45(3):282–291. doi:10.1097/SHK.0000000000000495
27. Hotchkiss RS, Monneret G, Payen D. Sepsis-induced immunosuppression: from cellular dysfunctions to immunotherapy. *Nat Rev Immunol*. 2013;13(12):862–874. doi:10.1038/nri3552
28. Luan YY, Dong N, Xie M, Xiao XZ, Yao YM. The significance and regulatory mechanisms of innate immune cells in the development of sepsis. *J Interferon Cytokine Res*. 2014;34(1):2–15. doi:10.1089/jir.2013.0042
29. Lee W, Park EJ, Kwon OK, et al. Dual peptide-dendrimer conjugate inhibits acetylation of transforming growth factor beta-induced protein and improves survival in sepsis. *Biomaterials*. 2020;246:120000. doi:10.1016/j.biomaterials.2020.120000
30. Cao C, Yu M, Chai Y. Pathological alteration and therapeutic implications of sepsis-induced immune cell apoptosis. *Cell Death Dis*. 2019;10(10):782. doi:10.1038/s41419-019-2015-1
31. Lai Y, Lin C, Lin X, Wu L, Zhao Y, Lin F. Identification and immunological characterization of cuproptosis-related molecular clusters in Alzheimer's disease. *Front Aging Neurosci*. 2022;14:932676. doi:10.3389/fnagi.2022.932676
32. Zhang S, Xie L, Zheng S, et al. Identification, Expression and Evolution of Short-Chain Dehydrogenases/Reductases in Nile Tilapia (Oreochromis niloticus). *Int J Mol Sci*. 2021;22(8):1.
33. Wang J, Han K, Zhang C, et al. Identification and validation of ADME genes as prognosis and therapy markers for hepatocellular carcinoma patients. *Biosci Rep*. 2021;41(5). doi:10.1042/BSR20210583.
34. Zhang N, Zhou B, Tu S. Identification of an 11 immune-related gene signature as the novel biomarker for acute myocardial infarction diagnosis. *Genes Immun*. 2022;23(7):209–217. doi:10.1038/s41435-022-00183-7
35. Barron-Gallardo CA, Garcia-Chagollan M, Moran-Mendoza AJ, et al. A gene expression signature in HER2+ breast cancer patients related to neoadjuvant chemotherapy resistance, overall survival, and disease-free survival. *Front Genet*. 2022;13:991706. doi:10.3389/fgene.2022.991706
36. Frances A, Cordelier P. The Emerging Role of Cytidine Deaminase in Human Diseases: a New Opportunity for Therapy? *Mol Ther*. 2020;28(2):357–366. doi:10.1016/j.ymthe.2019.11.026
37. Buhagiar-Labarchede G, Onclercq-Delic R, Vacher S, et al. Cytidine deaminase activity increases in the blood of breast cancer patients. *Sci Rep*. 2022;12(1):14062. doi:10.1038/s41598-022-18462-8
38. Thompson PW, Jones DD, Currey HL. Cytidine deaminase activity as a measure of acute inflammation in rheumatoid arthritis. *Ann Rheumatic Dis*. 1986;45(1):9–14. doi:10.1136/ard.45.1.9
39. Taysi S, Polat MF, Sari RA, Bakan E. Serum adenosine deaminase and cytidine deaminase activities in patients with systemic lupus erythematosus. *Clin Chem Lab Med*. 2002;40(5):493–495. doi:10.1515/CCLM.2002.085
40. Baines TJ, Clark A. Cytidine deaminase--a marker for pre-eclampsia? *Ann Clin Biochem*. 1985;22(Pt 4):420–422. doi:10.1177/000456328502200416
41. Boyum A, Tennfjord VA, Gran C, Lovhaug D, Oktedalen O, Brandtzaeg P. Bioactive cytidine deaminase, an inhibitor of granulocyte-macrophage colony-forming cells, is massively released in fulminant meningococcal sepsis. *J Infect Dis*. 2000;182(6):1784–1787. doi:10.1086/317596
42. Kumar S, Saxena J, Srivastava VK, et al. The Interplay of Oxidative Stress and ROS Scavenging: antioxidants as a Therapeutic Potential in Sepsis. *Vaccines*. 2022;10(10):1575. doi:10.3390/vaccines10101575
43. Bai Z, Li Y, Li Y, Pan J, Wang J, Fang F. Long noncoding RNA and messenger RNA abnormalities in pediatric sepsis: a preliminary study. *BMC Med. Genomics*. 2020;13(1):36. doi:10.1186/s12920-020-0698-x